

Universidade de São Paulo
Instituto de Matemática e Estatística
Bachalerado em Ciência da Computação

Giuliano Augusto Faulin Belinassi

Optimizing a Boundary Elements Method for Stationary Elastodynamic Problems Implementation with GPUs

São Paulo
Dezembro de 2017

Optimizing a Boundary Elements Method for Stationary Elastodynamic Problems Implementation with GPUs

Monografia final da disciplina
MAC0499 – Trabalho de Formatura Supervisionado.

Supervisor: Prof. Dr. Alfredo Goldman vel Lebman
[Cosupervisor: Prof. Dr. Marco Dimas Gubitoso]

São Paulo
Dezembro de 2017

Resumo

O Método de Elementos de Contorno é uma alternativa eficiente para modelar domínios ilimitados, podendo ser utilizado para simular vibrações no solo. Aplicando as abordagens descritas neste trabalho em uma implementação legada voltada a problemas estastodinâmicos estacionários, conseguimos um speedup de $20\times$ no tempo total de simulação utilizando uma Tesla K40c quando comparado com o programa original, e obtemos um speedup de $100\times$ no método responsável pela construção das matrizes H e G do problema dinâmico utilizando uma GeForce GTX 980. Com estes resultados é possível simular domínios com mais pontos de malha com uma quantidade menor de tempo.

Palavras-chave: Método de Elementos de Contorno, MEC, GPU, Computação Paralela, Computação de Alto Desempenho, Métodos Numéricos

Abstract

The Boundary Element Method (BEM) is a very efficient alternative for modeling unlimited domains, being useful to simulate soil vibrations. Applying the approach described in this work into a legacy implementation for stationary elastodynamic problems, we obtained a $20\times$ speedup in the total time of simulation using a Tesla K40c when compared to the original implementation, and a $100\times$ speedup in the routine responsible for building the H and G matrices of the dynamic problem with a GeForce GTX 980. With these results, it is possible to simulate domains with a higher number of mesh elements with a smaller amount of time.

Keywords: Boundary Elements Method, BEM, GPU, Parallel Computing, High Performance Computing, Numerical Methods

Contents

1	Introduction	1
1.1	Motivation	1
1.2	Research Approach	1
1.3	Objectives	2
1.4	Monograph Structure	2
2	Theoretical Background	3
2.1	The Boundary Elements Method	3
2.2	Gaussian Quadrature	3
2.3	LU Decomposition	5
2.4	Parallel Programming	7
2.4.1	CUDA Programming	8
2.5	Related Works	9
3	Development	11
3.1	Calling CUDA from Fortran 77	11
3.2	Ghmatecd Optimization and Parallelization	12
3.3	Ghmatece Optimization and Parallelization	15
3.4	Linear System Solving Optimization	16
3.5	Interec Paralelization and Optimization	16
3.5.1	Interec1 Parallelization	16
3.5.2	Interec2 Parallelization	17
4	Methods and Results	19
4.1	Methods	19
4.2	Results and Isolated Conclusions	20
4.2.1	Ghmatecd Routine	20
4.2.2	Ghmatece Routine	21
4.2.3	Rigid Routine	21
4.2.4	Linear System Solving Routine	22
4.2.5	Interec1 Routine	22

5	Final Conclusions	29
5.1	BEM Efficiency as a Computational Tool	29
5.2	As a Programmer	29
5.3	Future Works	30
A	Computers used in tests	31
	Bibliography	35

Chapter 1

Introduction

1.1 Motivation

Differential equations governing problems of Mathematical Physics have analytical solutions only in cases in which the domain geometry, boundary and initial conditions are fairly simple. Problems with arbitrary domains and fairly general boundary conditions can only be solved approximately, for example, by using numerical techniques. These techniques were strongly developed due to the presence of increasingly powerful computers, enabling the solution of complex mathematical problems.

The Boundary Element Method (BEM) is a very efficient alternative for modeling unlimited domains since it satisfies the Sommerfeld radiation condition, also known as geometric damping ([Katsikadelis, 2016](#)). This method can be used for numerically modeling the stationary behavior of 3D wave propagation in the soil and it is useful as a computational tool to aid in the analysis of soil vibration ([Dominguez, 1993](#)). A BEM based tool can be used for analyzing the vibration created by heavy machines, railway lines, earthquakes, or even to aid the design of offshore oil platforms.

With the advent of GPUs, several mathematical and engineering simulation problems were redesigned to be implemented into these massively parallel devices. However, first GPUs were designed to render graphics in real time, as a consequence, all the available libraries, such as OpenGL, were graphical oriented. These redesigns involved converting the original problem to the graphics domain and required expert knowledge of the selected graphical library.

NVIDIA noticed a new demand for their products and created an API called CUDA to enable the use of GPUs for general purpose programming. CUDA uses the concept of kernels, which are functions called from the host to be executed by GPU threads.

Regarding this work, this parallelization approach is useful because an analysis of a large domain requires a proportionally large number of mesh elements, and processing a single element have a high time cost. Doing such analysis in parallel reduces the computational time required for the entire program because multiple elements are processed at the same time. This advantage was provided by this research.

1.2 Research Approach

Although BEM has a very interesting mathematical background showing why it works, here we focus mainly on subjects pertinent to the computational nature of such method, such as algorithms used and implementation questions. Hence, we do not show any detailed

proof about any mathematical property of BEM or discuss how it can be used to solve a particular set of problems.

1.3 Objectives

The main objective of this work is to provide an optimized version of the code provided by Carrion (2002), either by (1) reducing the number of calculations, (2) improving cache usage, or (3) parallelizing costly routines. After all optimizations, the program must still yield acceptable results, that means we must still minimize errors caused by floating point imprecisions. Another objective is extend the number of mesh elements that the program can accept as input.

1.4 Monograph Structure

This document is presented in the following order: Chapter 2 presents an overview of theoretical background required, from the Boundary Elements Method formulation to the Gaussian Quadrature (used to calculate integrals numerically) and LU Decomposition (used to solve dense linear systems). Chapter 3 discusses all development process, including how routines were optimized and parallelized. Chapter 4 presents the methodology used in this research and the obtained results. Finally, Chapter 5 present conclusions from obtained data and some setbacks while developing in CUDA platform.

Chapter 2

Theoretical Background

2.1 The Boundary Elements Method

Without addressing details on BEM formulation, the Boundary Integral Equation for Stationary Elastodynamic Problems can be written as:

$$c_{ij}u_j(\xi, \omega) + \int_S t_{ij}^*(\xi, x, \omega)u_j(x, \omega)dS(x) = \int_S u_{ij}^*(\xi, x, \omega)t_j(x, \omega)dS(x) \quad (2.1)$$

After performing the geometry discretization, Equation (2.1) can be represented in matrix form as:

$$Hu = Gt \quad (2.2)$$

Functions $u_{ij}^*(\xi, x, \omega)$ and $t_{ij}^*(\xi, x, \omega)$ (called fundamental solutions) present a singular behavior when $\xi = x$ ordely $O(1/r)$, called weak singularity, and $O(1/r^2)$, called strong singularity, respectively. The r value represents the distance between x and ξ points. The integral of these functions, as seen in Eq. (2.1), will generate the G and H matrices respectively, as is shown in Eq. (2.2).

To overcome the mentioned problem in the strong singularity, one can use the artifice known as Regularization of the Singular Integral, expressed as follows:

$$\begin{aligned} c_{ij}(\xi)u_j(\xi, \omega) + \int_S [t_{ij}^*(\xi, x, \omega)_{\text{DYN}} - t_{ij}^*(\xi, x)_{\text{STA}}] u_j(x, \omega)dS(x) + \\ + \int_S t_{ij}(\xi, x)_{\text{STA}}u_j(x)dS(x) = \int_S u_{ij}^*(\xi, x, \omega)_{\text{DYN}}t_j(x, \omega)dS(x) \end{aligned} \quad (2.3)$$

Where DYN = Dynamic, STA = Static. The integral of the difference between the dynamic and static nuclei, the first term in Equation (2.3), does not present singularity when executed concomitantly as expressed because they have the same order in both problems.

2.2 Gaussian Quadrature

Some integrals can only be approximated by numerical methods such as the Gaussian quadrature, that means:

$$\int_{-1}^1 f(x)dx \approx \sum_{j=1}^n a_j f(x_j) \quad (2.4)$$

Where a_j are called weights and x_j are called abscissae, and these values can be computed using Legendre Polynomials, as introduced below.

Definition 1. Legendre Polynomials are given by the following recurrence:

$$\phi_j(x) = \begin{cases} 1, & \text{if } j = 0. \\ x, & \text{if } j = 1. \\ \frac{2j-1}{j}x\phi_{j-1}(x) - \frac{j-1}{j}\phi_{j-2}(x) & \text{if } j \in \mathbb{N} - \{0, 1\} \end{cases} \quad (2.5)$$

It can be shown that those polynomials have the following important properties:

Theorem 1. Legendre Polynomials satisfy the following properties (*Ascher e Greif, 2011*):

1. Orthogonality: for $i \neq j$, $\int_{-1}^1 \phi_i(x)\phi_j(x)dx = 0$.
2. Calibration: $|\phi_j(x)| \leq 1$ for any $-1 \leq x \leq 1$, and $\phi_j(1) = 1$.
3. Oscillation: $\phi_j(x)$ has degree equal to j and all its roots are inside $] - 1; 1[$.

The proof of such theorem is beyond the scope of this work. See *Ascher e Greif (2011)*.

Theorem 2. Let $q(x)$ be a polynomial of degree $< n$. Then $q(x)$ is orthogonal to $\phi_n(x)$, that is:

$$\int_{-1}^1 q(x)\phi_n(x)dx = 0 \quad (2.6)$$

Proof. Since $\{\phi_0, \phi_1, \dots, \phi_n\}$ is an orthogonal base of all polynomials of degree $\leq n$, then all polynomials of degree $\leq n$ can be written as linear combination of $\phi_0, \phi_1, \dots, \phi_n$. Since $q(x)$ degree is $< n$, then:

$$q(x) = \sum_{k=0}^{n-1} \alpha_k \phi_k(x) \quad (2.7)$$

with such information, just calculate:

$$\int_{-1}^1 q(x)\phi_n(x)dx = \int_{-1}^1 \left(\sum_{k=0}^{n-1} \alpha_k \phi_k(x) \right) \phi_n(x)dx = \sum_{k=0}^{n-1} \alpha_k \left(\underbrace{\int_{-1}^1 \phi_k(x)\phi_n(x)dx}_{0, \text{orthogonality}} \right) = 0 \quad (2.8)$$

□

These two theorems above are important for quadrature's precision. Let's now present the Gaussian Quadrature.

Let $r(x)$ be a polynomial of degree $< n$. The Gaussian Quadrature must satisfy the equation below with equality.

$$\int_{-1}^1 r(x)dx = \sum_{j=1}^n a_j r(x_j) \quad (2.9)$$

Let's now show a simple trick that can be done with Legendre Polynomials to enhance the quadrature precision. Let $p(x)$ be a polynomial of degree $< 2n$. If we divide $p(x)$ by $\phi_n(x)$, both quotient $q(x)$ and the remainder $r(x)$ have degree $< n$ because $\phi_n(x)$ have degree equal to n . That means:

$$p(x) = q(x)\phi_n(x) + r(x) \quad (2.10)$$

Integrating both sides:

$$\int_{-1}^1 p(x)dx = \underbrace{\int_{-1}^1 q(x)\phi_n(x)dx}_{0, \text{by Theorem 2}} + \int_{-1}^1 r(x)dx = \int_{-1}^1 r(x)dx \quad (2.11)$$

Let's now select the abscissae points wisely. If all x_j are zeroes of the Legendre Polynomials ($\phi_n(x_j) = 0$), then we would have:

$$p(x_j) = q(x_j) \underbrace{\phi_n(x_j)}_0 + r(x_j) = r(x_j) \quad (2.12)$$

This means that the quadrature is exact to any polynomial of degree up to $2n - 1$ if we could select the weights properly, thus the quadrature precision would be as good as we could approximate $f(x)$ by a polynomial of degree $2n - 1$. For the weight points, [Hildebrand \(1987\)](#) shows that one could use:

$$a_j = \frac{2(1 - x_j^2)}{(n + 1)^2(\phi_{n+1}(x_j))^2} \quad (2.13)$$

2.3 LU Decomposition

In many areas of science concerning numerical methods, it is necessary to find a solution that satisfies together many equations. In this subsection, we describe one of the most used algorithms to solve a specific kind of linear system of equations. Before showing such algorithms, a set of definitions and theorems are required to understand how it operates.

A *matrix* is denoted as an element of $\mathbb{C}^{m \times n}$, where m is the number of rows and n is the number of columns. A *vector* is an element of \mathbb{C}^m , where m is the number of rows. Notice that a vector is a single column matrix.

Definition 2. A *system of linear equations* is a equation of the form $Ax = b$, where $A \in \mathbb{C}^{m \times n}$, $b \in \mathbb{C}^n$ are known and $x \in \mathbb{C}^m$ is the only unknown in the equation.

Although the definition above is general to any linear system, here we will explore properties of linear systems characterized by a square and nonsingular matrix A .

Definition 3. A **square matrix** is such that the number of rows is equal to the number of columns. A matrix that is not square is called **rectangular**.

Definition 4. A matrix $A \in \mathbb{C}^{n \times n}$ is called **nonsingular** if and only if $Ax = 0 \Leftrightarrow x = 0$.

Linear systems that have nonsingular matrices have a unique solution, as demonstrated below.

Theorem 3. Let $A \in \mathbb{C}^{n \times n}$ be a nonsingular square matrix. Then the system $Ax = b$ admits a unique solution $x \in \mathbb{C}^n$.

Proof. Let A be a nonsingular square matrix and suppose, by absurd, that $Ax = b$ have two distinct solutions named x and y . Since y is also a solution, then $Ay = b$. But then $Ax - Ay = b - b = 0$. Isolating A we find that $A(x - y) = 0$. But since A is nonsingular, then by definition of nonsingularity we have that $(x - y) = 0$, implying that $x = y$. This result is an absurd because we supposed that x and y are distinct solutions. \square

There is also an interesting special case of square matrices, called triangular matrices. There are two types of triangular matrices, lower triangular and upper triangular.

Definition 5. *An upper triangular matrix is such that all elements below the main diagonal are 0. Analogously, a lower triangular matrix is such that all elements above the main diagonal are 0.*

The matrices below are examples of triangular matrices. At the left, we have an upper triangular matrix. At the right, we have a lower triangular matrix.

$$\begin{pmatrix} 1 & 2 & 3 \\ 0 & 4 & 5 \\ 0 & 0 & 6 \end{pmatrix} \quad \begin{pmatrix} 1 & 0 & 0 \\ 2 & 3 & 0 \\ 4 & 5 & 6 \end{pmatrix}$$

Systems of equations with triangular matrices have an interesting property that it can be solved with an $O(n^2)$ algorithm, as illustrated in algorithms 1 and 2.

Algorithm 1 Solves $Ax = b$, where A is a lower triangular nonsingular matrix. Replaces b with the result

```

1: procedure FORWARD_SUBSTITUTION( $A \in \mathbb{C}^{n \times n}$ ,  $b \in \mathbb{C}^n$ )
2:   for  $j := 1, n$  do
3:     if  $A[j][j] == 0$  then
4:       Error:  $A$  is singular.
5:      $b[j] \leftarrow b[j]/A[j][j]$ 
6:     for  $i := j + 1, n$  do
7:        $b[i] \leftarrow b[i] - A[i][j] * b[j]$ 

```

Algorithm 2 Solves $Ax = b$, where A is an upper triangular nonsingular matrix. Replaces b with the result

```

1: procedure BACKWARD_SUBSTITUTION( $A \in \mathbb{C}^{n \times n}$ ,  $b \in \mathbb{C}^n$ )
2:   for  $j := n, 1$  do
3:     if  $A[j][j] == 0$  then
4:       Error:  $A$  is singular.
5:      $b[j] \leftarrow b[j]/A[j][j]$ 
6:     for  $i := 1, j$  do
7:        $b[i] \leftarrow b[i] - A[i][j] * b[j]$ 

```

The question that rises now is how can we reduce a square nonsingular matrix A to triangular matrices. This is what LU decomposition with partial pivoting does, it decomposes A in three matrices $P^\top LU$, where P is a pivoting matrix, L is lower triangular and U is upper triangular. Briefly, a pivoting matrix is such that when operated with a matrix, it interchanges its columns; this is used to avoid divisions by 0 (Watkins, 2004). Algorithm 3 illustrates how A can be decomposed in such matrices.

Algorithm 3 Decomposes A in $P^\top LU$, P is a permutation matrix stored in a vector. Stores L and U over A .

```

1: procedure LU_PARTIAL_PIVOTING( $A \in \mathbb{C}^{n \times n}$ )
2:   Allocate  $P \in \mathbb{N}^{n-1}$ 
3:   for  $k := 1, n-1$  do
4:      $amax \leftarrow \max\{|A[k][k]|, |A[k+1][k]|, \dots, |A[n][k]|\}$ 
5:     if  $amax == 0$  then
6:       Error:  $A$  is singular.
7:      $m \leftarrow$  smaller integer  $\geq k$  that  $|A[m][k]| == amax$ 
8:      $P[k] \leftarrow m$ 
9:     if  $m \neq k$  then
10:      Swap column  $m$  and  $k$ 
11:     for  $i := k+1, n$  do
12:        $A[i][k] \leftarrow A[i][k]/A[k][k]$ 
13:     for  $j := k+1, n$  do
14:       for  $i := k+1, n$  do
15:          $A[i][j] \leftarrow A[i][j] - A[i][k] * A[k][j]$ 
16:   if  $A[n][n] == 0$  then
17:     Error:  $A$  is singular.

```

Using the fact that $A = P^\top LU$, one can solve $Ax = b$ by solving $P^\top LUx = b$. Since P is a permutation matrix, then its inverse $P^{-1} = P^\top$ (Watkins, 2004) and now one must solve $LUx = Pb$. Let $y = Ux$. Solving $Ly = Pb$ will result in a numerical value to y . Solving $Ux = y$ will finally assert x .

Since the cost of decomposing A into $P^\top LU$ is $O(n^3)$, the time required to compute $P^\top b$ is, naively, $O(n^2)$ and the time required to solve the two triangular systems is $O(n^2)$, then the cost of solving $Ax = b$ is $O(n^3)$.

2.4 Parallel Programming

Imagine the following scenario: You have to build a bridge to connect two parts of a city, named A and B, that are separated by a river. Let's say that if a single person builds this bridge from A to B, the time required to do so is t . How can we build this bridge faster? If we have another man building the same bridge in parallel to you but from B to A and connect it at the middle of the river, then the time required is $t/2$. This silly example captures the essence of parallel computing. How can we use multiple processors or multiple machines with some coordination to archive the same purpose? From this example comes the concept of speedup, as presented in the following definition.

Definition 6. Let T_1 be the time consumed to complete a task using one processor. Let $T_{||}$ be the time consumed to complete the same task using n processors. The speedup S_n is calculated by:

$$S_n = \frac{T_1}{T_{||}} \quad (2.14)$$

There are various computer architectures designed to handle parallel computing, as described by Flynn Taxonomy (Pacheco, 2011), but remarks are necessary to two architectures.

1. SIMD: Stands for Single Instruction, Multiple Data. This refers to vectorized processors allowing a single operation to be executed in a vector content. Examples are Intel SSE and GPUs, although GPUs are not a pure SIMD, as described later.
2. MIMD: Stands for Multiple Instruction, Multiple Data. This refers to independent multicore systems, capable of executing tasks asynchronously. in MIMD is located both shared memory and distributed memory systems. Shared memory systems are an example of it, where various processors read and write to a shared memory. For such systems, a collection of directives called OpenMP can be used to explore its parallel capabilities with little changes in the original code. (Pacheco, 2011)

An important concept regarding parallel computing is the concept of processes and threads. A process is an operating system (OS) abstraction that allows a program to have the illusion that it monopolizes the entire CPU (Love, 2005). Every process has at least one execution flow, which is named thread. Modern OS can handle multiple threads within a process, allowing many different executions flows in the same process. (Tanenbaum, 2009)

Although OpenMP uses simple pragmas to take advantage of multiple CPUs in a shared memory system by creating multiple threads within a process, GPUs require severe modifications in the original code to run in such devices. NVIDIA developed CUDA for this purpose.

2.4.1 CUDA Programming

CUDA is an acronym to Compute Unified Device Architecture and it is an extension to C++ language that allows running general purpose code in NVIDIA GPUs. Its execution is divided into a host (CPU) and device (GPU) parts. For the device part, CUDA uses the concept of kernels, which are functions called from the host to be executed by GPU threads. The memory space is also separated between the host and the device, and data must be manually transferred from host to device in order to allow a device to access them, or from device to host to retrieve results computed by the GPU. Figure 2.2 illustrates the execution flow of a CUDA program.

CUDA kernels are organized into a set of blocks composed of a set of threads that cooperate with each other. The number of threads within a block and the number of blocks are specified at the launch moment, thus it can be adjusted to match the problem input size. The GPU's memory hierarchy also reflects this organization (Kirk e Wen-Mei, 2016), since it is divided into four types:

1. Registers: Private to each thread, it is used to hold frequently accessed data.
2. Shared Memory: It is a low latency memory shared between all threads within a block.
3. Constant Memory: A read-only memory that provides short latency and high bandwidth access.
4. Global Memory: A memory located outside the GPU processor chip. It can be accessed by all threads, but it is slower than all before-mentioned memories. It is the most abundant memory in the device.

It must be highlighted that all threads may not run in parallel since it is limited to the amount of Streaming Multiprocessors (SM) the device has. Without entering in details, an SM is what schedules a set of 32 threads called Warps, executing each instruction in a SIMD fashion. Hence, the number of threads running in parallel is limited by the amount of SM

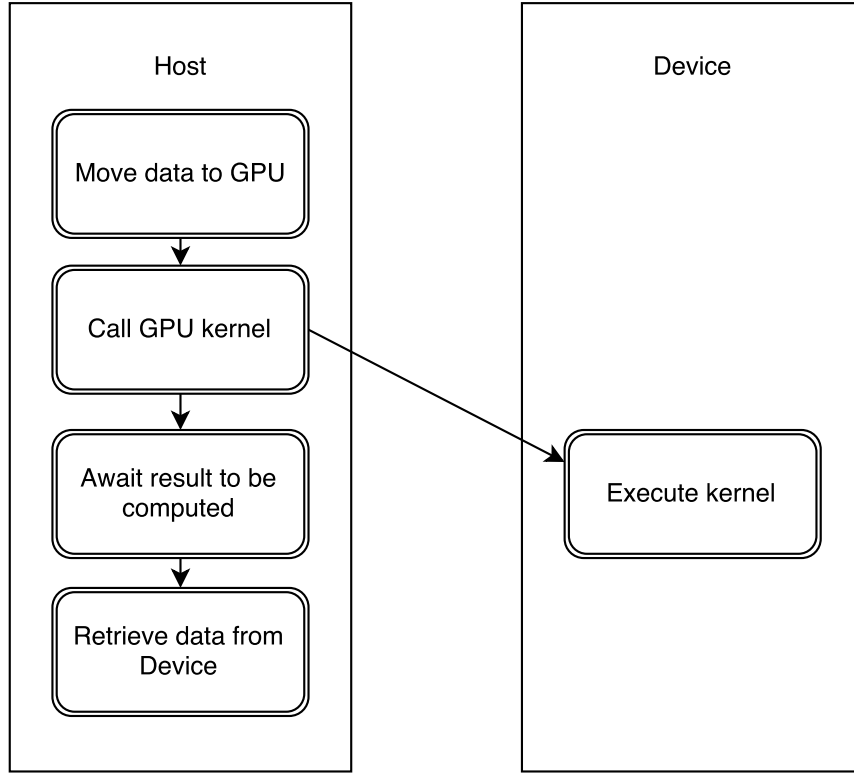


Figure 2.1: A typical CUDA execution flow.

available in the GPU. Because a GPU contains multiples SM, it is not considered a pure SIMD device.

In order to maximize the efficiency of a CUDA application, the programmer needs to minimize the memory transfer between CPU and GPU and explore any parallelism structure of the problem, as discussed in [devTalk \(2012\)](#).

2.5 Related Works

As GPUs became famous by its massively parallel capabilities and applications were developed to explore its potential, there is no surprise that researchers would use GPUs to accelerate Boundary Elements Method implementations.

[Torky e Rashed \(2017\)](#) presented an implementation for generating both H and G matrices of equation 1.2 with GPU acceleration using two CUDA kernels: One for computing the G matrix and one for the H matrix.

While assembling both H and G matrices, the authors managed to archive a speedup of 25 times and kept the H matrix in GPU memory to avoid memory transfers between device and host. With regard to solving the linear system, they obtained a speedup of 1300 times. Both results were obtained using an Intel Core i7-3770 paired GeForce GTX 970.

As for precision, there is no further discussion other than the usage of 10 points for the Gaussian Quadrature and that both CPU and GPU processed data in exactly the same manner and with reliable accuracy.

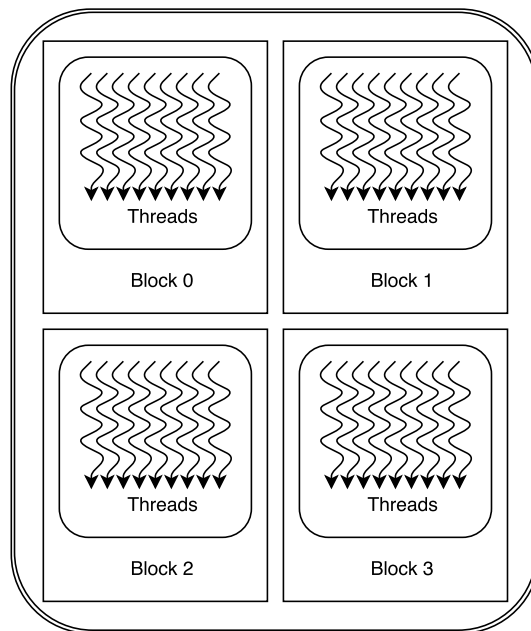


Figure 2.2: *Organization of a kernel execution with 9 threads per block and 4 blocks.*

Chapter 3

Development

The first goal of the project was to compile and execute the code with at least one sample. While doing these, we found a few issues such as:

- The original code provided by Carrion had issues common to legacy code. It depended on some features offered by Compaq Visual Fortran, thus the code needed modifications to be able to compile with the GFortran compiler. The code also had indentation issues and used several GOTO statements to execute simple tasks such as looping because of limitations imposed by Fortran 77.
- There were no automated tests for the program.
- Fortran has a feature called implicit variable declaration that showed to be error-prone because the code had a bug due to a misspelled variable in a file named `Solfundif.for` (the RDN variable was misspelled DRN), and the compiler did not complain about the uninitialized variable.
- There was a need to call CUDA code from Fortran to avoid a complete rewrite of the application in C or C++. The Portland Group (PGI) provides a paid CUDA Fortran compiler, so another solution was required.
- The original code only used static memory allocation for loading all data. This resulted in the following problems: (1) Huge memory usage for small inputs because the application does not know the memory requirement to load the data, and (2) A limit of 2Gb of memory for the total of statically allocated variables (Corden, 2010).

After all those issues were addressed, a parallel optimization of BEM began by analyzing the sequential code provided. Gprof, a profiling tool by GNU, revealed the two most time-consuming routines: `Ghmatecd` and `Nonsingd`, with 60.9% and 58.3% of the program total elapsed time, respectively. Since most calls to `Nonsingd` were performed inside `Ghmatecd`, most of the parallelization effort was focused on that last routine.

3.1 Calling CUDA from Fortran 77

Although The Portland Group (PGI) provides a CUDA Fortran compiler, it is not free-ware software and thus might increase the application development costs. An alternative to this is to create C++ functions that are callable from Fortran and use CUDA C++ to program the kernels.

Since GFortran appends an underscore to all compiled Fortran subroutines, manually appending it to a C routine makes it visible to Fortran. Since Fortran also passes all arguments as reference, then the C routine needs to expect a pointer to a variable rather than the variable itself. Now, to call C++ from Fortran it is necessary to just wrap the function with `extern "C"` clause, as exemplified below.

```
1 extern "C"{
2   void callable_from_fortran_(int* a, int* b){
3     printf("%d\n", (*a) + (*b));
4   }
5 }
```

```
1   PROGRAM CALL_C
2     INTERFACE
3       SUBROUTINE callable_from_fortran(a, b)
4         IMPLICIT NONE
5         INTEGER a, b
6       END SUBROUTINE
7     END INTERFACE
8
9     CALL callable_from_fortran(40, 2)
10  END PROGRAM CALL_C
```

It must be highlighted that matrices in Fortran are stored in column-major order and indexed from 1, whereas in C and C++ they are stored in line-major order and indexed from 0. This means that when accessing the position $A(i, j)$ from a Fortran matrix in C, one must access $A[j-1][i-1]$.

3.2 Ghmatedcd Optimization and Parallelization

Ghmatedcd is a routine developed to create both the H and G matrices for the dynamic problem described in Equation (2.2). It does so by making several calls to `Nonsingd`, a routine that uses the Gaussian Quadrature as described in Chapter 2.2 to compute the integral of the dynamic part in Equation (2.1); and `Sing_de`, a routine that implements the artifice described by Equation (2.3).

At first, we did some optimization to the original sequential code to remove unnecessary computations or memory copy. Ghmatedcd's code had additional matrices used in the computations that dependency analysis showed to be unnecessary. There was also a vectorial product that was computed for each column of H and G that were recomputed in other routines, thus it was moved to a separate function called `Normvec` and its result passed to Ghmatedcd.

We also optimized `Nonsingd` routine by removing all calls to a procedure named `Gauleg` that were used to compute the abscissae and weight points of the Gaussian Quadrature. These points are always the zeroes of the Legendre Polynomials and there is no need to compute them more than once in the entire program, hence the result of `Gauleg` can just be passed to `Nonsingd`.

Algorithm 1 shows the pseudocode for the Ghmatedcd subroutine. Let n be the number of mesh elements and m the number of boundary elements. Ghmatedcd builds matrices H and G by computing smaller 3×3 matrices returned by `Nonsingd` and `Sing_de`.

Algorithm 4 Creates $H, G \in \mathbb{C}^{(3m) \times (3n)}$

```

1: procedure GHMATECD
2:   for  $j := 1, n$  do
3:     for  $i := 1, m$  do
4:        $ii := 3(i - 1) + 1; jj := 3(j - 1) + 1$ 
5:       if  $i == j$  then
6:          $Gelement, Helement \leftarrow \text{Sing\_de}(i)$  ▷ two  $3 \times 3$  complex matrices
7:       else
8:          $Gelement, Helement \leftarrow \text{Nonsingd}(i, j)$ 
9:        $G[ii : ii + 2][jj : jj + 2] \leftarrow Gelement$ 
10:       $H[ii : ii + 2][jj : jj + 2] \leftarrow Helement$ 

```

There is no interdependency between all iterations of the loops in lines 2 and 3, so all iterations can be computed in parallel. With OpenMP, this can be done with a simple `pragma for` statement. Since typically a modern high-end CPU have 8 cores, even a small number of mesh elements generate enough workload to use all CPUs resources if this strategy alone is used. On the other hand, a typical GPU contain thousands of processors, hence even a considerable large amount of elements may not generate a workload that consumes all the device's resources. Since `Nonsingd` is the cause of the performance bottleneck of `Ghmatedcd`, the main effort was put to implementing an optimized version of `Ghmatedcd`, called `Ghmatedcd_Nonsingd`, that only computes the `Nonsingd` case in the GPU, and leave `Sing_de` to be computed in the CPU after the computation of `Ghmatedcd_Nonsingd` is completed. The pseudocode in Algorithm 5 pictures a new strategy where `Nonsingd` is also computed in parallel. Let g be the number of Gauss quadrature points.

Algorithm 5 Creates $H, G \in \mathbb{C}^{(3m) \times (3n)}$

```

1: procedure GHMATECD_NONSINGD
2:   for  $j := 1, n$  do
3:     for  $i := 1, m$  do
4:        $ii := 3(i - 1) + 1; jj := 3(j - 1) + 1$ 
5:       Allocate Hbuffer and Gbuffer, buffer of matrices  $3 \times 3$  of size  $g^2$ 
6:       if  $i \neq j$  then
7:         for  $y := 1, g$  do
8:           for  $x := 1, g$  do
9:              $Hbuffer(x, y) \leftarrow \text{GenerateMatrixH}(i, j, x, y)$ 
10:             $Gbuffer(x, y) \leftarrow \text{GenerateMatrixG}(i, j, x, y)$ 
11:             $Gelement \leftarrow \text{SumAllMatricesInBuffer}(Gbuffer)$ 
12:             $Helement \leftarrow \text{SumAllMatricesInBuffer}(Hbuffer)$ 
13:             $G[ii : ii + 2][jj : jj + 2] \leftarrow Gelement$ 
14:             $H[ii : ii + 2][jj : jj + 2] \leftarrow Helement$ 
15: procedure GHMATECD_SING_DE
16:   for  $i := 1, m$  do
17:      $ii := 3(i - 1) + 1$ 
18:      $Gelement, Helement \leftarrow \text{Sing\_de}(i)$ 
19:      $G[ii : ii + 2][ii : ii + 2] \leftarrow Gelement$ 
20:      $H[ii : ii + 2][ii : ii + 2] \leftarrow Helement$ 
21: procedure GHMATECD
22:   Ghmatedcd_Nonsingd()
23:   Ghmatedcd_Sing_de()

```

The `Ghmatedcd_Nonsingd` routine can be implemented as a CUDA kernel. In a CUDA block, $g \times g$ threads are created to compute in parallel the two nested loops in lines 2 and 3, allocating spaces in the shared memory to keep the matrix buffers `Hbuffer` and `Gbuffer`. Since these buffers contain matrices of size 3×3 , nine of these $g \times g$ threads can be used to sum all matrices, because one thread can be assigned to each matrix entry, unless $g < 3$. Note that g is also upper-bounded by the amount of shared memory available in the GPU. Launching $m \times n$ blocks to cover the two nested loops in lines 2 to 3 will generate the entire H and G without the `Sing_de` part. The `Ghmatedcd_Sing_de` routine can be parallelized with a simple OpenMP `Parallel for` clause, and it will compute the remaining H and G .

A careful examination of `Sing_de` lead us to conclude that, algorithmically, it is very similar to `Nonsingd` with a special logic to overcome singularity issues. If we merge both procedures in one, then there would be no need to compute the diagonal of H and G using the CPU. Algorithm 6 captures this idea.

Algorithm 6 Creates $H, G \in \mathbb{C}^{(3m) \times (3n)}$

```

1: procedure GHMATECD
2:   for  $j := 1, n$  do
3:     for  $i := 1, m$  do
4:        $ii := 3(i - 1) + 1; jj := 3(j - 1) + 1$ 
5:       Allocate  $Hbuffer$  and  $Gbuffer$ , buffer of matrices  $3 \times 3$  of size  $g^2$ 
6:       for  $y := 1, g$  do
7:         for  $x := 1, g$  do
8:            $Hbuffer(x, y) \leftarrow \text{GenerateMatrixH}(i, j, x, y)$ 
9:            $Gbuffer(x, y) \leftarrow \text{GenerateMatrixG}(i, j, x, y)$ 
10:          if  $i == j$  then
11:             $\text{OvercomeSingularity}(i, \&Hbuffer(x, y), \&Gbuffer(x, y))$ 
12:           $Gelement \leftarrow \text{SumAllMatricesInBuffer}(Gbuffer)$ 
13:           $Helement \leftarrow \text{SumAllMatricesInBuffer}(Hbuffer)$ 
14:           $G[ii : ii + 2][jj : jj + 2] \leftarrow Gelement$ 
15:           $H[ii : ii + 2][jj : jj + 2] \leftarrow Helement$ 

```

Algorithm 6 can be implemented as a CUDA kernel analogously as `Ghmatecd_Nonsingd`. This strategy has the advantage of only using the GPU to compute the entire H and G and there are no idle blocks as in Algorithm 5, but tests show a significant loss of precision in this version when compared to the previous one.

3.3 Ghmatece Optimization and Parallelization

Ghmatece is a routine developed to create both the H and G matrices for the static problem described in equation (2.2). Except for RIGID routine, a procedure designed to calculate H diagonal by considering the rigid body movement, it is very similar to Ghmatecd routine as described by Algorithm 7.

Algorithm 7 Creates $H, G \in \mathbb{R}^{(3m) \times (3n)}$

```

1: procedure GHMATECE
2:   for  $j := 1, n$  do
3:     for  $i := 1, m$  do
4:        $ii := 3(i - 1) + 1; jj := 3(j - 1) + 1$ 
5:       if  $i == j$  then
6:          $Gelement, Helement \leftarrow \text{Singge}(i)$  ▷ two  $3 \times 3$  real matrices
7:       else
8:          $Gelement, Helement \leftarrow \text{Nonsinge}(i, j)$ 
9:          $G[ii : ii + 2][jj : jj + 2] \leftarrow Gelement$ 
10:         $H[ii : ii + 2][jj : jj + 2] \leftarrow Helement$ 
11:   Rigid( $H$ )
12: procedure RIGID( $H$ )
13:   for  $i := 1, m$  do
14:     for  $j := 1, n$  do
15:        $ii := 3(i - 1) + 1; jj := 3(j - 1) + 1$ 
16:       if  $i \neq j$  then
17:          $H[ii : ii + 2][ii : ii + 2] \leftarrow H[ii : ii + 2][ii : ii + 2] + H[ii : ii + 2][jj : jj + 2]$ 

```

The parallelization technique presented in Algorithm 5 can be applied to Ghmatece because Nonsinge operates in the same way as Nonsingd, but it computes the integral of the static nuclei in Equation (2.1). Unfortunately, since Singge makes 4 calls to Nonsinge, the strategy presented in algorithm 6 cannot be deployed efficiently because it would generate too much workload to a group of blocks.

For the RIGID procedure, it has no interdependency between lines and thus it can be parallelized using the `!$OMP PARALLEL DO` pragma.

3.4 Linear System Solving Optimization

In order to compute all regions surface forces and displacements, a linear system can be assembled from the matrices H and G from the dynamic problem, which means solving:

$$Ax = b \quad (3.1)$$

where A is a square nonsingular complex matrix. As described in section 2.3, the LU decomposition with partial pivoting can be deployed to solve it.

The original code used a sequential implementation provided by Compaq within a routine called CGESV. In order to explore multiple CPUs, a library called OpenBLAS implements this routine taking advantage of multicore architectures.

A Library named MAGMA implements the LU decomposition with GPU acceleration within a function named `magma_cgesv_gpu` that shows good results for this application.

3.5 Interec Paralelization and Optimization

Interec is a routine designed to calculate displacements and tensions over internal points. Such routine can be broken into two routines: Interec1, a routine designed to calculate a vector $d \in \mathbb{C}^{3L}$ containing the displacements; and Interec2, a routine that calculates a vector $s \in \mathbb{C}^{9L}$ containing the tensions, where L is the number of internal points and m is the number of boundary elements. Algorithm 8 sketches this routine.

3.5.1 Interec1 Parallelization

Although Interec1 calls Nonsingd, its results differs significantly from Ghmatecd because the inputs are different.

Let now d_i be the section $d[ii : ii + 2]$, that is, d_i is a vector of size 3. Analogously, Let b_j and u_j be $b[jj : jj + 2]$ and $u[jj : jj + 2]$. Let H_{ij}^{element} and G_{ij}^{element} be the two results from the Nonsingd routine from the step i, j . Then line 6 of Algorithm 8 can be expressed mathematically as:

$$d_i = \sum_{j=1}^m G_{ij}^{\text{element}} b_j - H_{ij}^{\text{element}} u_j \quad (3.2)$$

This can be reorganized as:

$$d_i = \left(\sum_{j=1}^m G_{ij}^{\text{element}} b_j \right) - \left(\sum_{j=1}^m H_{ij}^{\text{element}} u_j \right) \quad (3.3)$$

Algorithm 8 Creates $d \in \mathbb{C}^{3L}$, $s \in \mathbb{C}^{9L}$

```

1: procedure INTEREC1
2:   for  $j := 1, m$  do
3:     for  $i := 1, L$  do
4:        $ii := 3(i - 1) + 1; jj := 3(j - 1) + 1$ 
5:        $G^{\text{element}}, H^{\text{element}} \leftarrow \text{Nonsingd}(i, j)$ 
6:        $d[ii : ii + 2] \leftarrow d[ii : ii + 2] + G^{\text{element}} \times b[ii : ii + 2] - H^{\text{element}} \times b[ii : ii + 2]$ 
7: procedure INTEREC2
8:   for  $i := 1, L$  do
9:     for  $j := 1, m$  do
10:       $ii := 3(i - 1) + 1; jj := 3(j - 1) + 1$ 
11:       $Z, S \leftarrow \text{Sigmaec}(i, j)$ 
12:      for  $k = 1, 3$  do
13:         $kk := 9(j - 1) + 3(k - 1) + 1$ 
14:         $s[kk : kk + 2] \leftarrow s[kk : kk + 2] + D[k] \times d[kk : kk + 2] - S[k] \times d[kk : kk + 2]$ 
15: Interec1()
16: Interec2()
```

Lets define two matrices $H \in \mathbb{C}^{(3L) \times (3m)}$ and $G \in \mathbb{C}^{(3L) \times (3m)}$ such that $H_{ij} = H_{ij}^{\text{element}}$ and $G_{ij} = G_{ij}^{\text{element}}$. Now the entire vector d can be expressed as:

$$d = Gb - Hu \quad (3.4)$$

Matrices H and G in Eq. (3.4) can be assembled analogously as in Algorithm 6 just without special logic to overcome singularity issues (remove lines 10 and 11 of such algorithm). After that, just use cuBLAS to multiply Hu and Gb , and subtract the resulting vectors. Algorithm 9 illustrates this approach.

Algorithm 9 Creates $d \in \mathbb{C}^{3L}$

```

1: procedure INTEREC1
2:   for  $j := 1, m$  do
3:     for  $i := 1, L$  do
4:        $ii := 3(i - 1) + 1; jj := 3(j - 1) + 1$ 
5:       Allocate  $Hbuffer$  and  $Gbuffer$ , buffer of matrices  $3 \times 3$  of size  $g^2$ 
6:       for  $y := 1, g$  do
7:         for  $x := 1, g$  do
8:            $Hbuffer(x, y) \leftarrow \text{GenerateMatrixH}(i, j, x, y)$ 
9:            $Gbuffer(x, y) \leftarrow \text{GenerateMatrixG}(i, j, x, y)$ 
10:       $Gelement \leftarrow \text{SumAllMatricesInBuffer}(Gbuffer)$ 
11:       $Helement \leftarrow \text{SumAllMatricesInBuffer}(Hbuffer)$ 
12:       $G[ii : ii + 2][jj : jj + 2] \leftarrow Gelement$ 
13:       $H[ii : ii + 2][jj : jj + 2] \leftarrow Helement$ 
14:  $d \leftarrow Hu - Gb$ 
```

3.5.2 Interec2 Parallelization

Due to the deadline, the Interec2 routine was not parallelized using GPUs, although an OpenMP version is implemented.

Chapter 4

Methods and Results

4.1 Methods

Matrix norms were used to assert the correctness of our results. Let $A \in \mathbb{C}^{m \times n}$. Watkins (2004) defines matrix 1-norm as:

$$\|A\|_1 = \max_{1 \leq j \leq n} \sum_{i=1}^m |a_{ij}| \quad (4.1)$$

All norms have the property that $\|A\| = 0$ if and only if $A = 0$. Let u and v be two numerical algorithms that solve the same problem, but in a different way. Now let y_u be the result computed by u and y_v be the result computed by v . The *error* between these two values can be measured computing $\|y_u - y_v\|$. The error between CPU and GPU versions of H and G matrices was computed by calculating $\|H_{cpu} - H_{gpu}\|_1$ and $\|G_{cpu} - G_{gpu}\|_1$.

Gfortran and CUDA 8.0 were used to compile the application. The main flags used in Gfortran were `-Ofast -march=native -funroll-loops -flto`. The flags used in CUDA nvcc compiler were: `-use_fast_math -O3 -Xptxas -opt-level=3 -maxrregcount=32 -Xptxas -allow-expensive-optimizations=true`.

For experimenting, there were four data samples as shown in Table 4.1. Each routine defines the label `gpu` in its context, but the `cpu` label means that the routine was executed only in CPU.

Before any data collection, a warm up procedure is executed, which consists of running the application with the sample three times without getting any result. Afterward, all experiments were executed 30 times per sample. Each execution produced a file with total time elapsed, where a script computed averages and standard deviations for all experiments.

The graphs labels consist of the implementation name concatenated with the number of OpenMP threads used, for example, `cpu8` implies that only the CPU was used with 8 OpenMP threads. All its points are the mean of the time in seconds of 30 executions, and the errorbars illustrate a 95% confidence interval.

The number of threads used were defined considering the number of CPU cores the testing machine has. We used two machines for the tests, BrucutuIV and Venus, as defined in Appendix A

GPU total time was computed by the sum of 5 elements: (1) total time to move data to GPU, (2) launch and execute the kernel, (3) elapsed time to compute the result, (4) time to move data back to main memory, (5) time to compute any remaining parts in the CPU. The elapsed time was computed in seconds with the OpenMP library function `OMP_GET_WTIME`. This function calculates the elapsed wall clock time in seconds with double precision. All

Table 4.1: *Data experiment set*

Number of Mesh elements	240	960	2160	4000	14400
Number of Boundary elements	100	400	900	1600	6400

experiments set the Gauss Quadrature Points to 8 and the number of Internal Points to 10.

4.2 Results and Isolated Conclusions

4.2.1 Ghmatecd Routine

This routine has three parallel implementations: (1) Using only CPU threads (`cpu`); (2) Using GPU for the nonsingular part and the CPU for the singular part, as described by Algorithm 5 (`gpu`); (3) Using GPU for both singular and nonsingular parts, as described by Algorithm 6 (`gpu_sing`).

BrucutuIV Data

The logarithmic scale graphic in Figure 4.1 illustrates the results for BrucutuIV. We removed the points from the graph that represents the sequential data for legibility.

The speedup acquired in the 14400 mesh elements sample with `cpu48`, `cpu24`, `gpu8` and `gpu_sing1` with respect to the sequential algorithm are 25, 19, 22 and 22 respectively in BrucutuIV. For this sample we can see that a single Tesla K40 was faster than a single Xeon E5-2650 v4, but slower than two of those processors.

Notice that with respect to time, `gpu8` and `cpu_sing1` behaves very similarly, but there is an interesting observation about the error (computed as described in Section 4.1), as illustrated in Figure 4.2.

Since there is an error gap in the H matrix between the `gpu8` and `gpu_sing1`, it suggests that most errors concentrate around computation of the singular case and it is more sensible to floating point errors, thus better precision is required here.

As a conclusion, the presented method can be used to accelerate the overall performance of the mentioned routine, and a load balancer can be developed from these results for even higher speedups because of two items: (1) similar computational time elapsed between `gpu_sing1` and `cpu24` in the 14400 sample, and (2) the fact that `gpu_sing1` only uses one CPU thread, allowing other threads to also consume workload.

Venus Data

Here the obtained speedup was 3, 100 and 100 respectively for the `cpu4`, `gpu4` and `gpu_sing1` on the 4000 mesh sample. We could not run the 14400 sample because it requires around 16 Gigabytes of RAM, but the machine only had 8 Gigabytes. In this machine, the GeForce GTX980 was faster than the AMD A10-7700K even for the 960 sample. This was due to lower CPU-GPU memory transfer latency. The logarithm graphic at Figure 4.3 illustrates the results.

The errors followed the same behavior as discussed in BrucutuIV Data section, as illustrated in Figure 4.4. Notice that the errors in H are worse when compared to BrucutuIV.

From these data, we can conclude that the presented method can also accelerate the performance in the case that there is a low number of CPU cores available, and such CPU cores can be allocated to compute the singular case to reduce errors.

4.2.2 Ghmatece Routine

This routine has two parallel implementations: (1) Using only CPU threads (`cpu`); (2) Using GPU for the nonsingular part and the CPU for the singular part (`gpu`), as presented by the technique in Algorithm 5. Here we present the results for the Ghmatece routine without the Rigid part. We present in this way because we present a detailed analysis of the Rigid routine also in this chapter.

BrucutuIV Data

The logarithm graphic in Figure 4.5 illustrates the results for BrucutuIV. The speedup acquired in the 14400 mesh elements sample with `cpu24`, `cpu48`, and `gpu8` with respect to the sequential algorithm are 15, 19, and 13 respectively in BrucutuIV. For this sample, we can see that the Tesla K40 was slower than a single Xeon E5-2650 v4. Although Ghmatece routine is similar to Ghmatecd, it does fewer computations and thus offloading this task alone to the GPU may not be attractive.

As for the error, the 14400 was the only sample that had errors greater than 10^{-5} . Since the $\|\bullet\|_1$ grows as the number of matrix rows increases, this result was expected. Figure 4.6 illustrates the results.

As a conclusion, the GPU can be used to speedup this routine, but a load balancer is required for a better resource usage because of: (1) Smaller speedup when compared to the CPU implementation with 24 threads and (2) better than the theoretical possible speedup with only 8 CPU threads.

Venus Data

The logarithm graphic in Figure 4.7 illustrates the results for Venus. From the figure, we can conclude that for all samples but the 240 meshes there were speedups. The speedup acquired in the 4000 mesh elements sample with `cpu4` and `gpu4` with respect to the sequential algorithm are 2 and 32 respectively. As for the error, all results were below 10^{-6} .

As a conclusion, for this hardware, the presented implementation provides acceleration if the number of meshes is large enough.

4.2.3 Rigid Routine

We only present a parallel implementation of this routine using the CPU due to the low time consumption of it when compared to the other analysed routines. We only present the BrucutuIV data because the 14400 sample was the only one that provides a meaningful information about the elapsed time.

BrucutuIV Results

Figure 4.8 illustrates the results. The speedup acquired in the 14400 mesh elements sample with `cpu24` and `cpu48` with respect to the sequential implementation are 12 and 13 respectively in BrucutuIV. Since all those results but the sequential are below 1s and this routine is called only once in the entire program, there is no requirement for vast improvements here.

4.2.4 Linear System Solving Routine

This routine has two parallel implementations: (1) Using OpenBLAS CGESV (cpu) and (2) Using MAGMA's `cgesv_gpu` routine (gpu).

BrucutuIV results

Figure 4.9 illustrates the results for BrucutuIV. The acquired speedup in the 14400 mesh elements sample in `cpu24`, `cpu48`, `gpu1` and `gpu48` with respect to the sequential algorithm are 10, 7, 29 and 30, respectively.

From these results, we can conclude that MAGMA's `cgesv_gpu` can be used to accelerate programs that require solving dense linear systems. Notice the slowdown when comparing `cpu24` with `cpu48`. We could not identify its causes, but we suspect of cache related issues because there are two processors in this machine, thus cache invalidation may be a problem.

Venus results

Figure 4.10 illustrates the results for Venus. The acquired speedup in the 4000 mesh elements sample in `cpu4` and `gpu4` are 2 and 38, and the BrucutuIV conclusions about this routine also prevails in this machine.

4.2.5 Interec1 Routine

Venus Results

The logarithm graphic in Figure 4.11 illustrates the results for Venus. From the figure, we can conclude that for all samples there were speedups. The speedup acquired in the 4000 mesh elements sample with `cpu4` and `gpu1` with respect to the sequential algorithm are 3 and 17 respectively. As for the error, all results were below 10^{-6} .

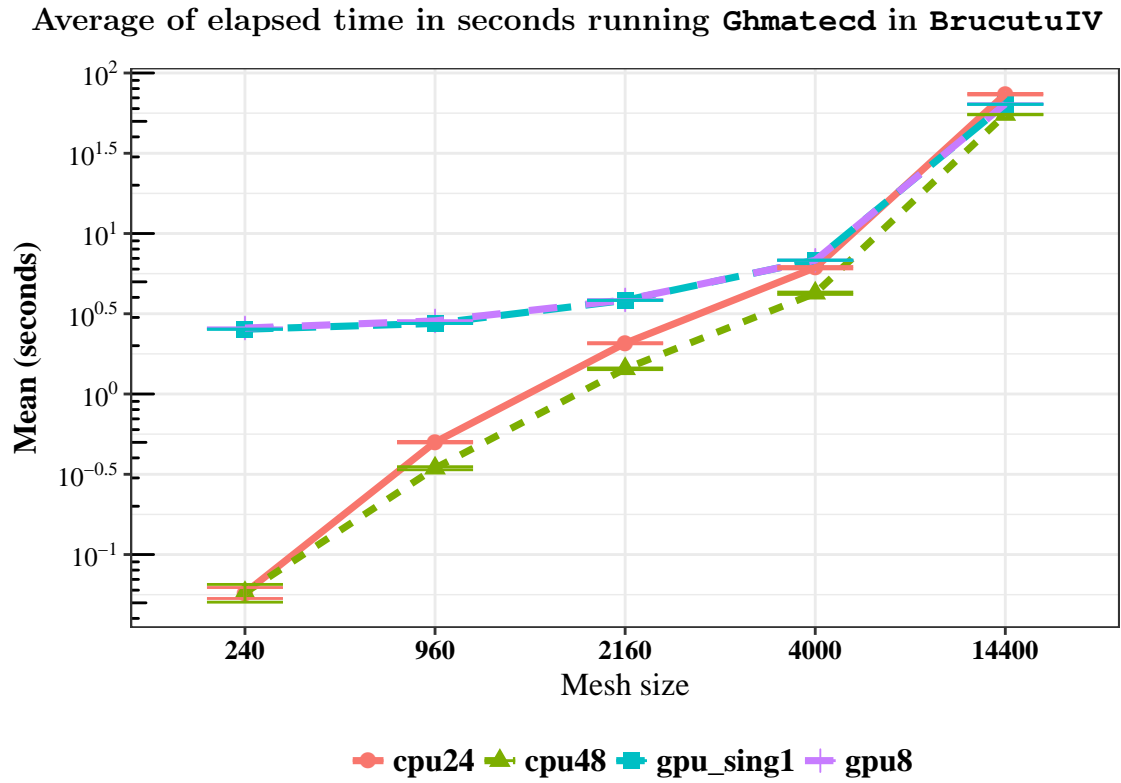


Figure 4.1: *Ghmatecd*: Time elapsed by each implementation in *BrucutuIV*

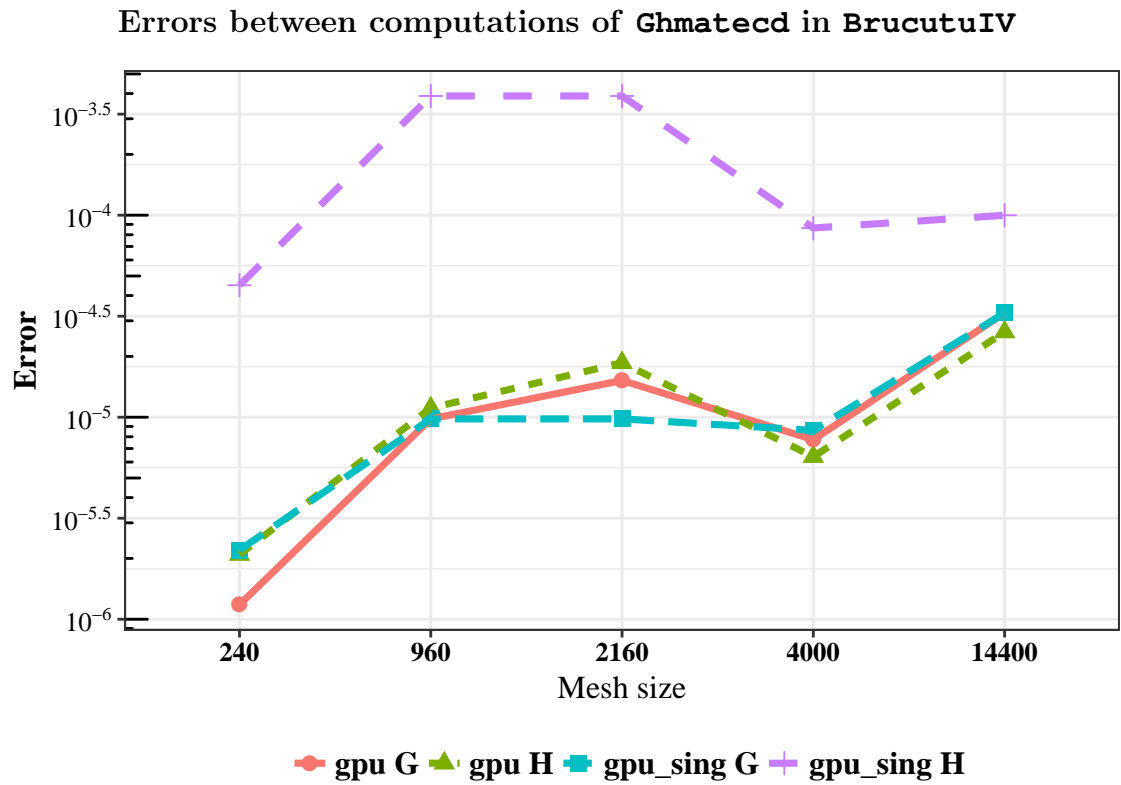


Figure 4.2: *Ghmatecd*: Error of each implementation compared with the CPU implementation in *BrucutuIV*

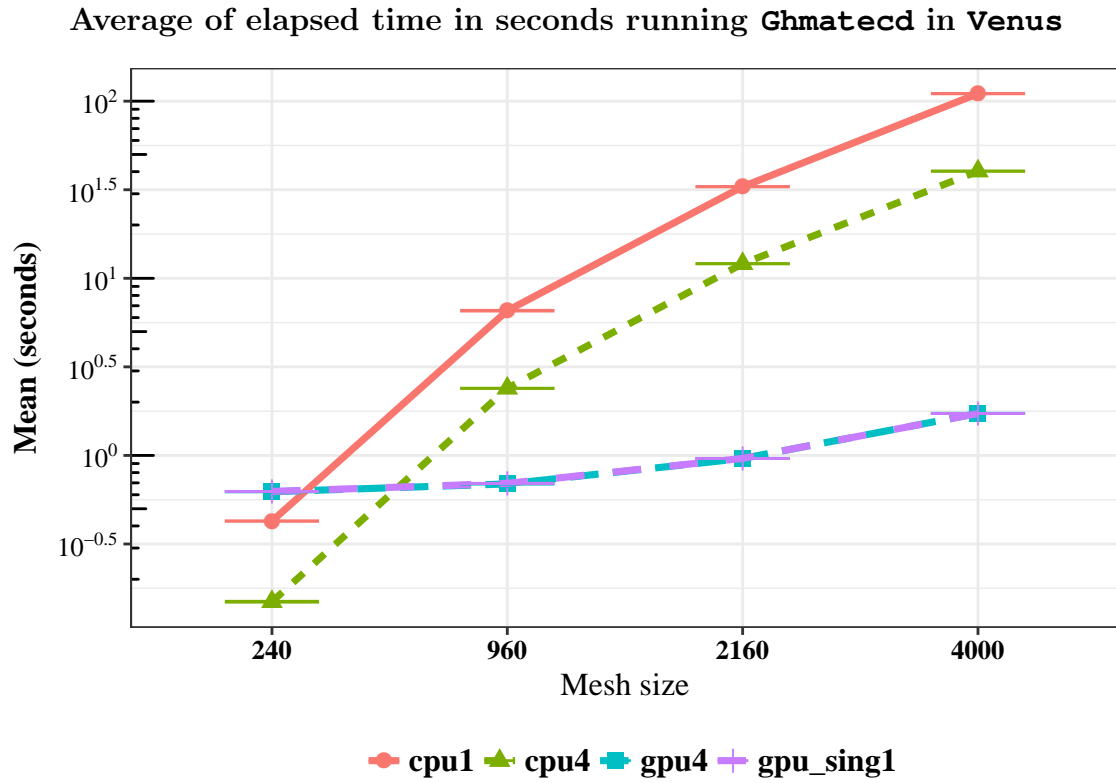


Figure 4.3: *Ghmatecd*: Time elapsed by each implementation in Venus

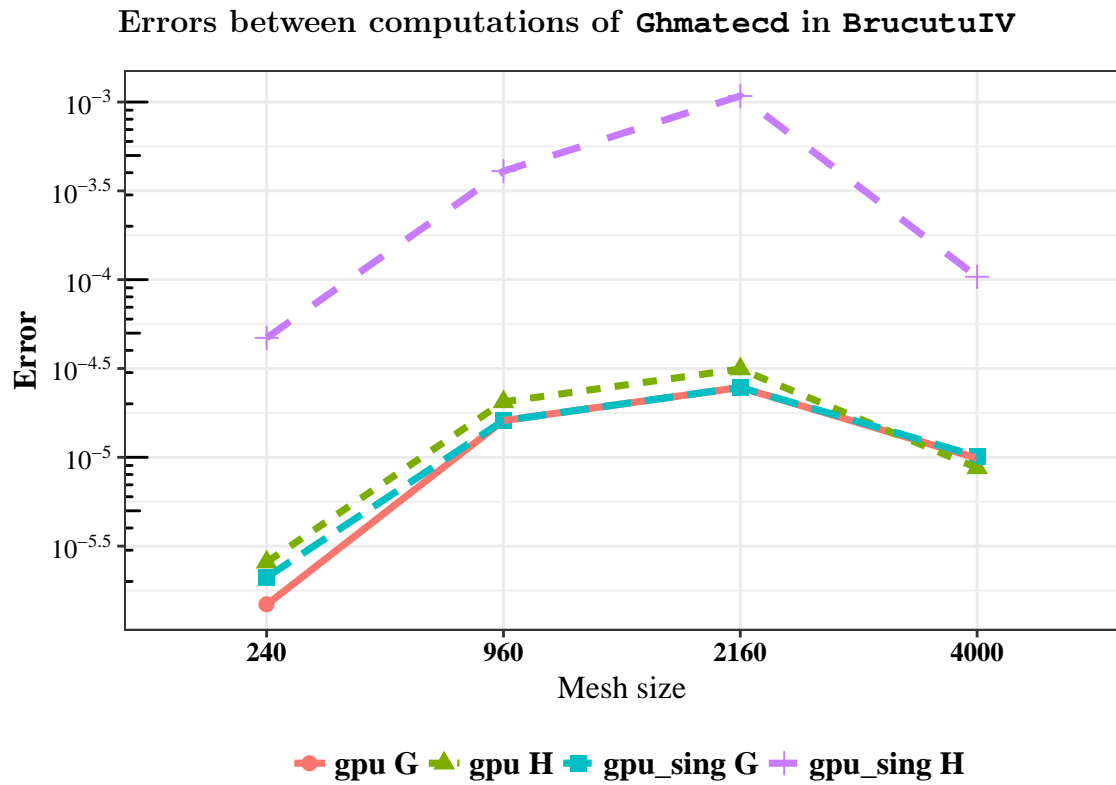


Figure 4.4: *Ghmatecd*: Error of each implementation compared with the CPU implementation in Venus

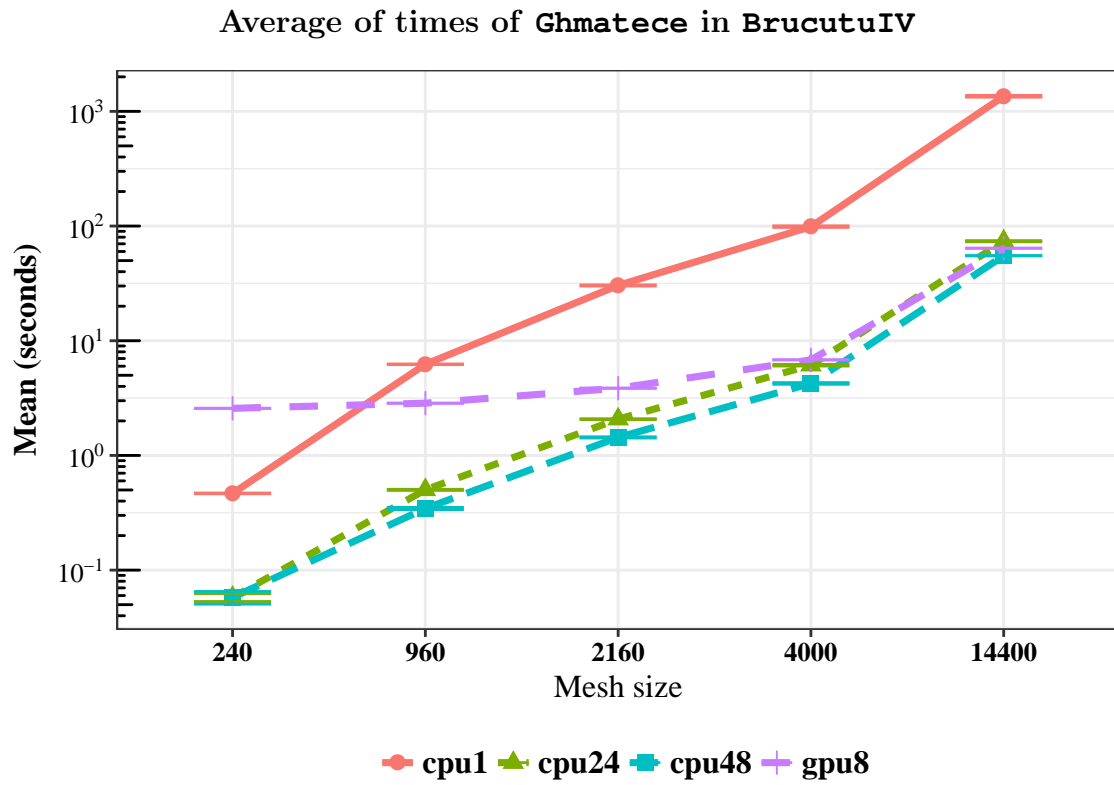


Figure 4.5: *Ghmatece*: Time elapsed by each implementation in *BrucutuIV*

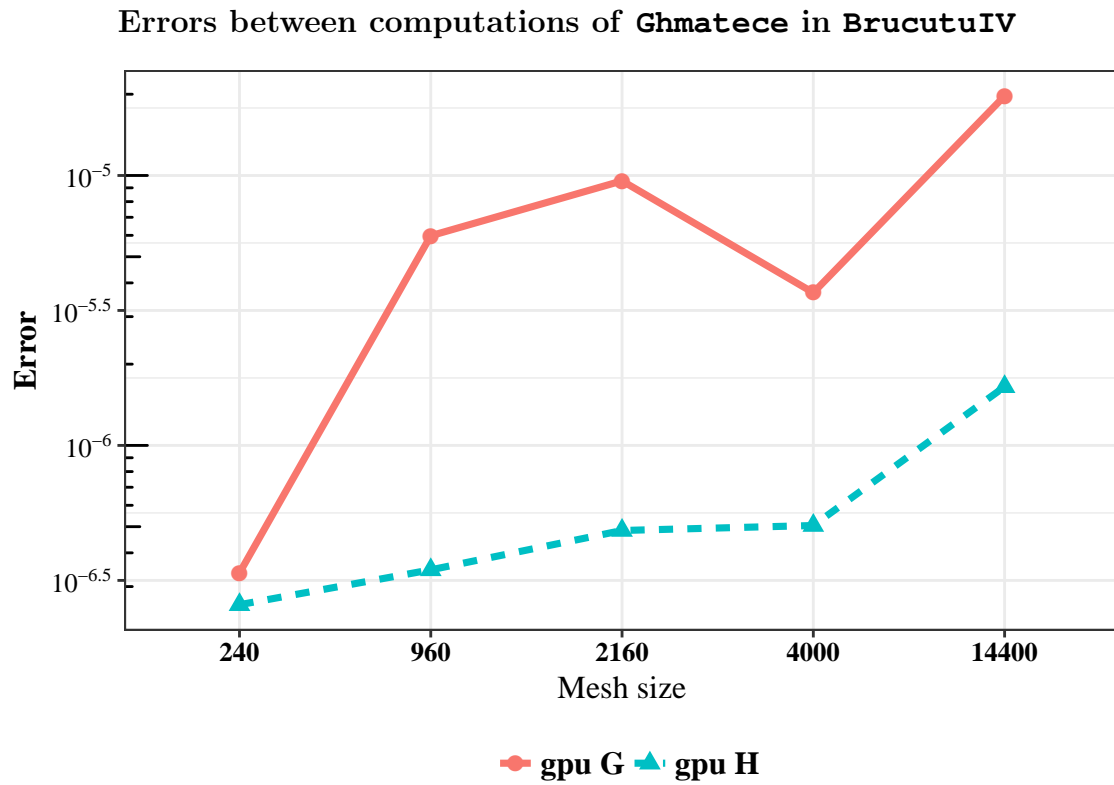


Figure 4.6: *Ghmatece*: Error of each implementation compared with the CPU implementation in *BrucutuIV*

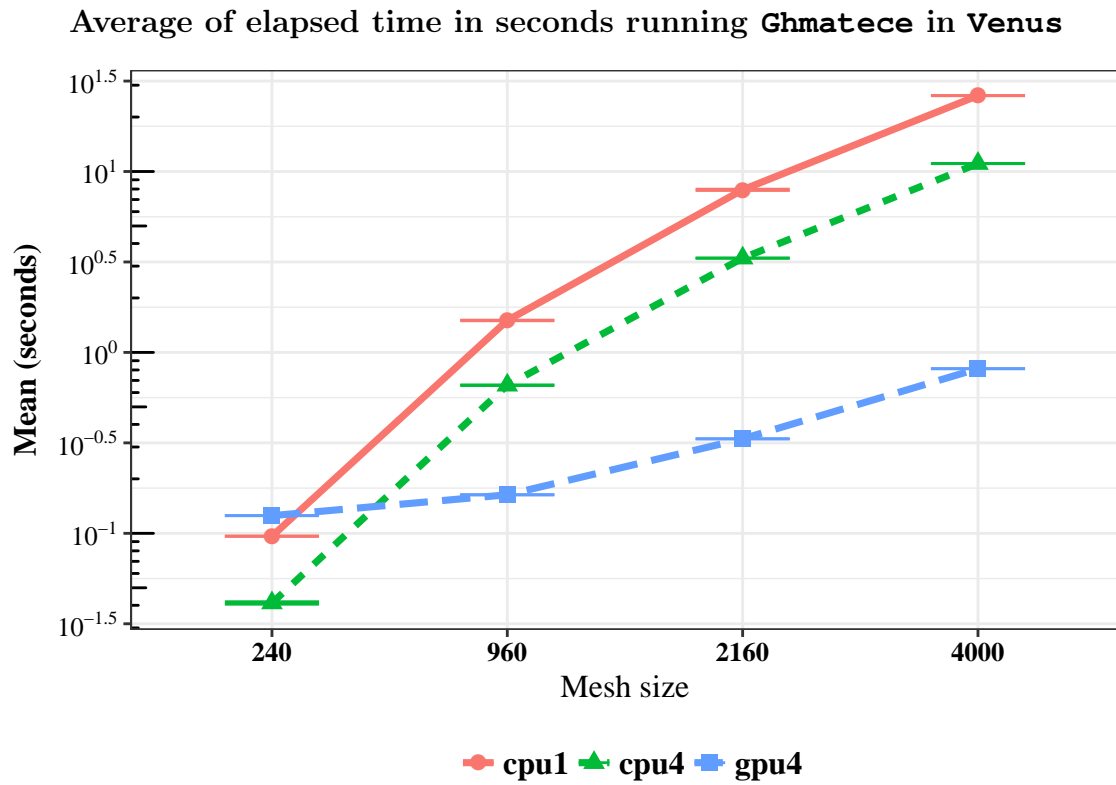


Figure 4.7: *Ghmatece*: Time elapsed by each implementation in *Venus*

Average of elapsed time in seconds running **Rigid** in **BrucutuIV**

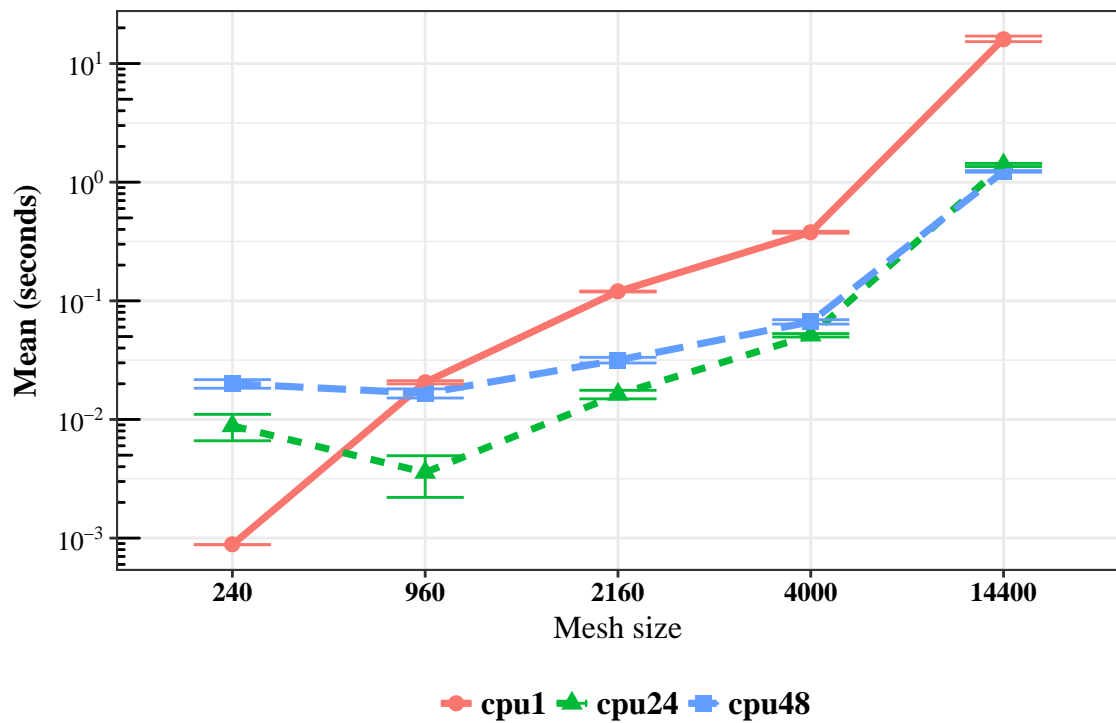
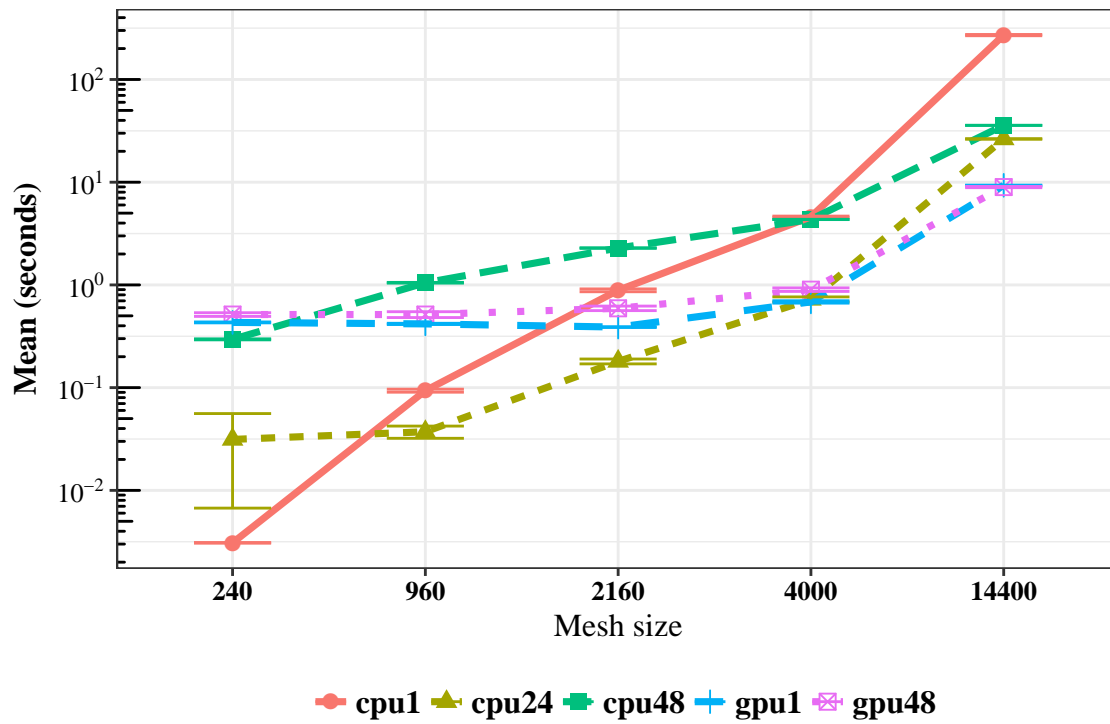
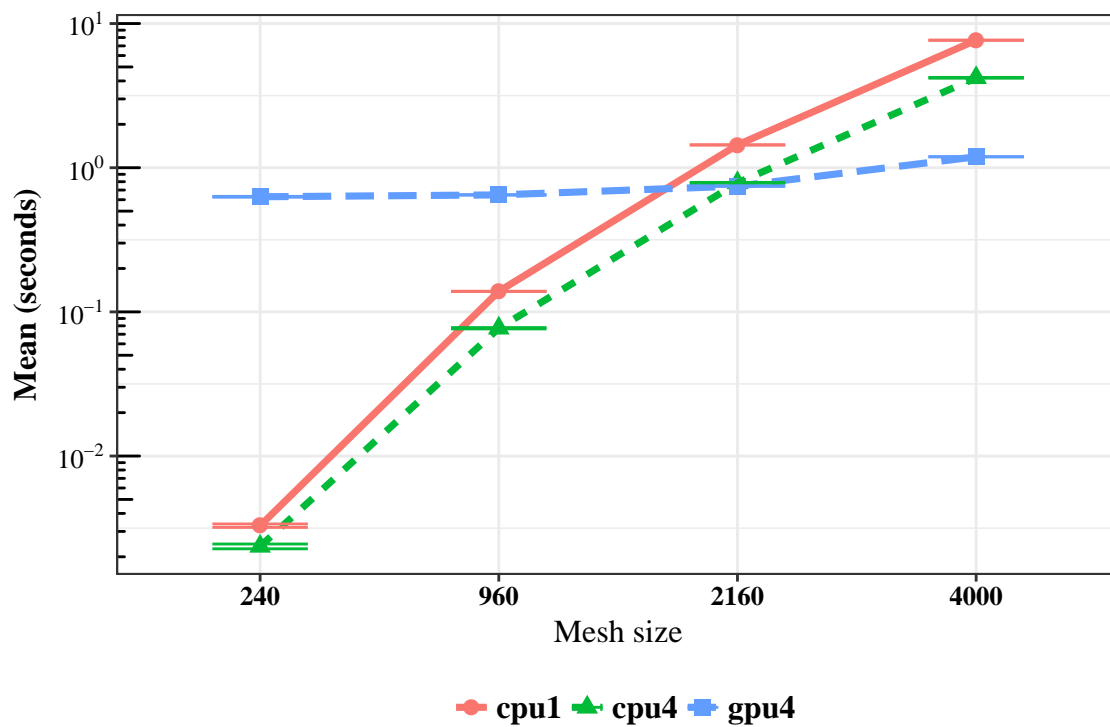


Figure 4.8: *Rigid*: Time elapsed by each implementation in *BrucutuIV*

Average of elapsed time in seconds running **Linsolve** in **BrucutuIV**Figure 4.9: *Linsolve*: Time elapsed by each implementation in *BrucutuIV*Average of elapsed time in seconds running **Linsolve** in **Venus**Figure 4.10: *Linsolve*: Time elapsed by each implementation in *Venus*

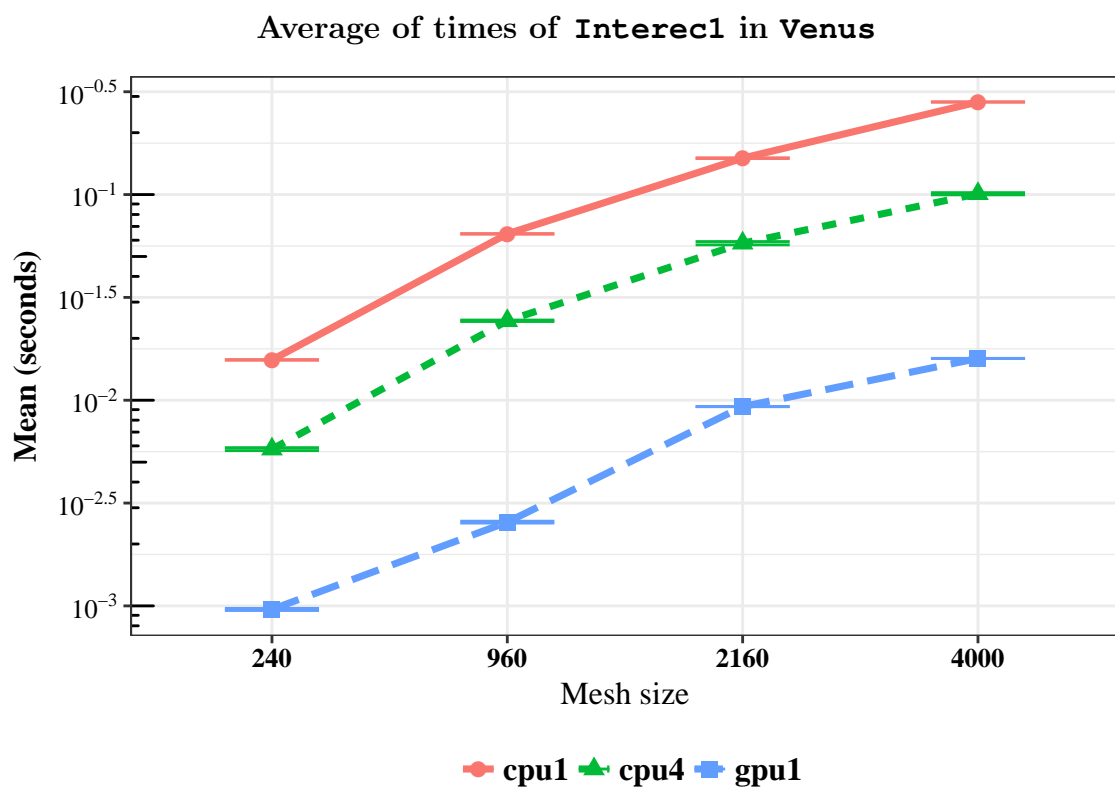


Figure 4.11: *Interec1*: Time elapsed by each implementation in Venus

Chapter 5

Final Conclusions

5.1 BEM Efficiency as a Computational Tool

We can discuss the efficiency of BEM as a computational tool from the obtained results.

Since all costly routines of BEM can be parallellized, its implementation can take advantage of multicore machines and GPUs to reduce the time required in simulations.

Since the GeForce GTX 980 provided stunning results in *Venus*, a home computer paired with such GPU can execute the simulation faster without investing into a more costly server. Similar results were published in WSCAD-WIC conference, earning second place in the best paper category (Belinassi *et al.*, 2017).

When compared to the original program, the total time elapsed in the simulation was reduced to a margin that is feasible for bigger mesh numbers such as the 14400 sample, as shown in Figure 5.1. It is possible to archive even more speedups if a load balancer is implemented in a way that it can use both CPU and GPU in parallel.

If there is a major concern about errors in the simulation, perhaps caution is required when offloading the task to the GPU, as the mainly graphic on Figure 4.2 indicates.

As a final conclusion, the program can now be used to simulate cases where the original couldn't because of time constraints or unnecessary memory usage. It also has no issues running in modern Linux distributions once all project dependencies are installed.

5.2 As a Programmer

Adding features regarding to a technology that did not exist in the time period of the program's development was a challenge at first mainly because of sparse support for the original language nowadays. Sure, calling C from Fortran in the way we presented enabled the current solution, but what if it couldn't be done in that way? That could be the case for even older systems.

Also, implementing numeric algorithms is no easy task because minor mistakes on a variable cause an absurd impact on results, but without crashing the program. Using automated tests to isolate the faulty routine is determinant for solving the problem because such incorrect results propagate to subsequent routines, causing the problem's source to be lost. Once such routine is detected, GDB is useful to determine what variable is the cause of such undesired behaviour. Tests are important and must not be underestimated.

As for the GPU development, testing an code is painful as we are unable to run `X11` and `cuda-gdb` in the same GPU simultaneously. Additionally, sometimes a `SEGFault` in a CUDA kernel caused the computer to hang, requiring a complete reboot of the machine.

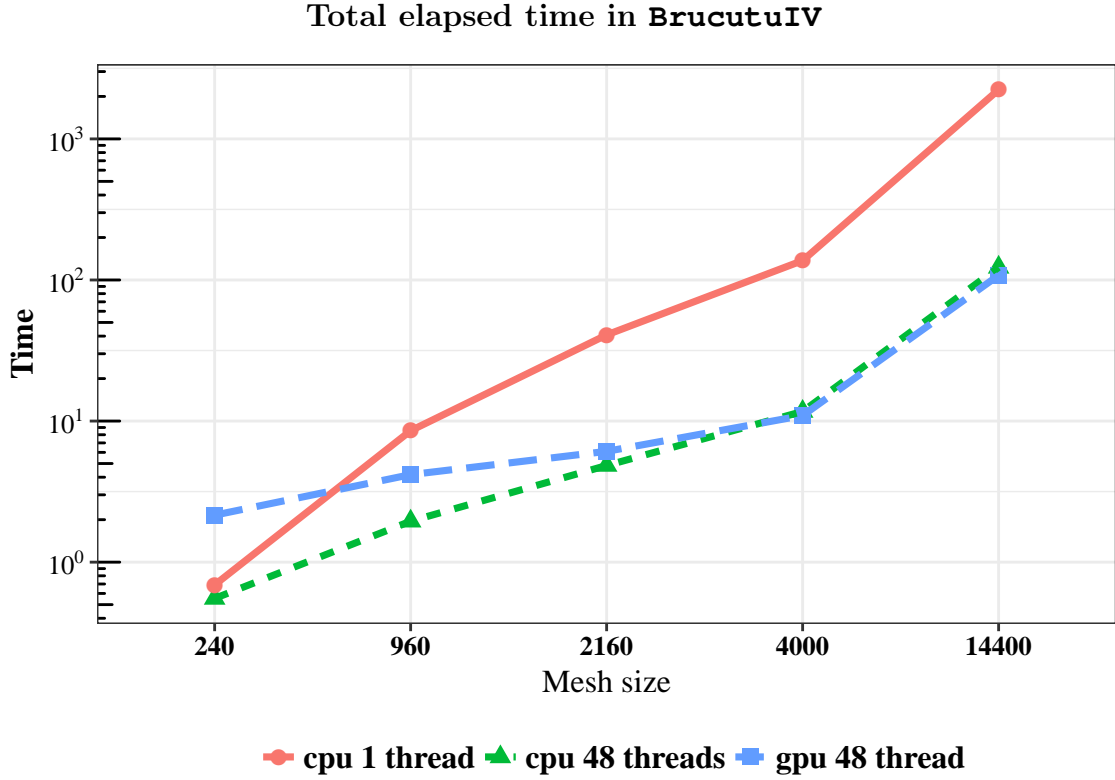


Figure 5.1: Total elapsed time in BrucutuIV. One data per sample

One last item is that it is not possible to allocate multiple arrays in CUDA’s shared memory dynamically, requiring pointer magic to allocate multiple arrays into a single array. All these points require improvements.

5.3 Future Works

The presented implementation can still be improved. A load balancer can be developed for distributing workload between CPU and GPU for constructing the H and G matrices from Ghmatece and Ghmatecd routines for better speedups.

The linear system solving routine can run quicker simply by keeping the H matrix in GPU memory. This is not already implemented due to the structure of the current program, a refactoration is necessary.

A better parallel strategy for reducing the matrix (as illustrated by the function SumAllMatricesInBuffer of Algorithms 5 and 6) is required for better speedups. This can lead to even better speedups.

An implementation of Interec2 in GPUs can be attractive for samples with a large number of internal points, providing better speedups to the application.

Appendix A

Computers used in tests

- Computer BrucutuIV:

Processor: 2x Intel(R) Xeon(R) CPU E5-2650 v4 @ 2.20GHz

Cores: 24

Threads: 48

Number of OpenMP threads used in experiments: 1, 8, 24, 48

GPU: NVIDIA Corporation GK110BGL [Tesla K40c]

RAM: 378G

Version of GFortran: 4.9.2

Topology: Figure [A.1](#)

- Computer Venus:

Processor: AMD A10-7700K Radeon R7, 10 Compute Cores 4C+6G

Cores: 4

Threads: 4

Number of OpenMP threads used in experiments: 1, 4

RAM: 8G

GPU: NVIDIA Corporation GM204 [GeForce GTX 980]

Version of GFortran: 5.4.0

Topology: Figure [A.2](#)



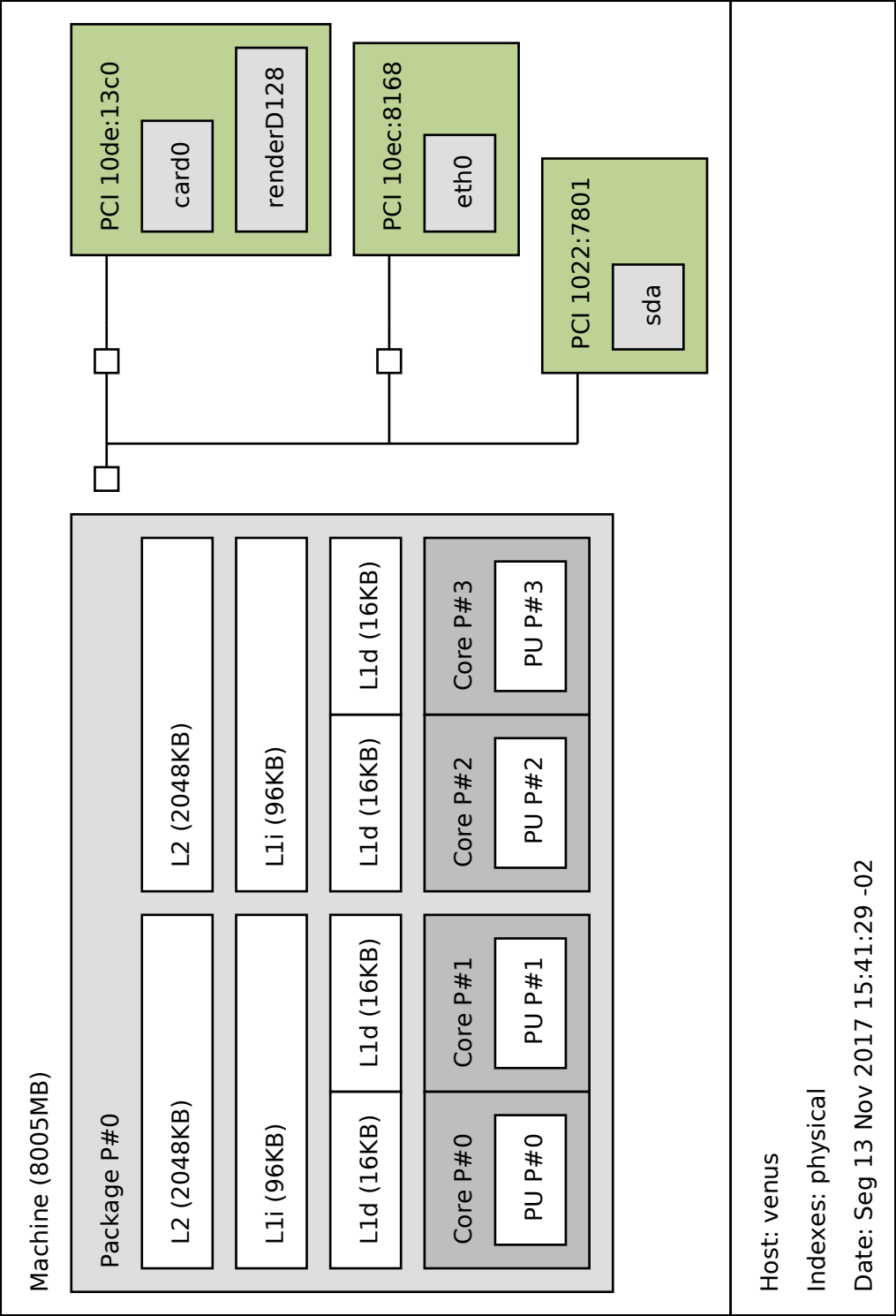


Figure A.2: Topology of Venus.

Bibliography

Ascher e Greif(2011) Uri M Ascher e Chen Greif. *A first course on numerical methods*. SIAM. Citado na pág. 4

Belinassi et al.(2017) Giuliano Belinassi, Rodrigo Siqueira, Ronaldo Carrion, Alfredo Goldman e Marco Gubitoso. Optimizing a boundary elements method for stationary elastodynamic problems implementation with gpus. *WSCAD–WIC*, 18:51–56. Citado na pág. 29

Carrion(2002) Ronaldo Carrion. *Uma Implementação do Método dos Elementos de Contorno para problemas Viscoelastodinâmicos Estacionários Tridimensionais em Domínios Abertos e Fechados*. Tese de Doutorado, Universidade Estadual de Campinas. Citado na pág. 2

Corden(2010) Martyn Corden. Avoiding relocation errors when building applications with large global or static data on intel64 linux. <https://software.intel.com/en-us/articles/avoiding-relocation-errors-when-building-applications-with-large-global-or-static-data-on-intel64/>, 2010. Accessed: 2017-11-23. Citado na pág. 11

devTalk(2012) NVIDIA devTalk. How to optimize data transfers in cuda c/c++. <https://devblogs.nvidia.com/parallelforall/how-optimize-data-transfers-cuda-cc/>, 2012. Accessed: 2017-08-06. Citado na pág. 9

Dominguez(1993) Jose Dominguez. *Boundary elements in dynamics*. Wit Press. Citado na pág. 1

GNU() GNU. Gnu binutils. <https://www.gnu.org/software/binutils/>. Accessed: 2017-05-08. Citado na pág. 11

Hildebrand(1987) Francis Begnaud Hildebrand. *Introduction to numerical analysis*. Courier Corporation. Citado na pág. 5

Katsikadelis(2016) John T Katsikadelis. *The Boundary Element Method for Engineers and Scientists: Theory and Applications*. Academic Press. Citado na pág. 1

Kirk e Wen-Mei(2016) David B Kirk e W Hwu Wen-Mei. *Programming massively parallel processors: a hands-on approach*. Morgan kaufmann. Citado na pág. 8

Love(2005) Robert Love. *Linux Kernel Development (2Nd Edition) (Novell Press)*. Novell Press. ISBN 0672327201. Citado na pág. 8

Pacheco(2011) Peter Pacheco. *An introduction to parallel programming*. Elsevier. Citado na pág. 7, 8

Tanenbaum(2009) Andrew Tanenbaum. *Modern operating systems*. Pearson Education, Inc.,. Citado na pág. 8

- Torky e Rashed(2017)** Ahmed A Torky e Youssef F Rashed. Gpu acceleration of the boundary element method for shear-deformable bending of plates. *Engineering Analysis with Boundary Elements*, 74:34–48. Citado na pág. [9](#)
- Watkins(2004)** David S Watkins. *Fundamentals of matrix computations*, volume 64. John Wiley & Sons. Citado na pág. [6](#), [7](#), [19](#)